Broatch Jacobi, JA.; Guardiola García, C.; Pla Moreno, B.; Bares Moreno, P. (2015). A direct transform for determining the trapped mass on an internal combustion engine based on the in-cylinder pressure resonance phenomenon. Mechanical Systems and Signal Processing. 62-63:480-489. doi:10.1016/j.ymssp.2015.02.023.

A direct transform for determining the trapped mass on an internal combustion engine based on the in-cylinder pressure resonance phenomenon

Alberto Broatch[a], Carlos Guardiola[a], Benjamín Pla[a], Pau Bares[a,*]

[a]*CMT-Motores Térmicos, Universitat Politècnica de València*

Abstract

It has lately been demonstrated that the resonance of the in-cylinder pressure may be used for inferring the trapped mass in an internal combustion engine. The resonance frequency changes over time as the expansion stroke takes place, and hence time-frequency analysis techniques may be used for determining the instantaneous frequency. However, time-frequency analysis has different problems when obtaining the spectral content of the signal, e.g. Short-Time Fourier Transform dilutes the frequency spectrum, and the Wigner Distribution creates cross terms that difficult its interpretation. In addition, time-frequency analysis requires a significant computational burden. This paper presents a direct transform, based on the resonance phenomenon, which obtains the trapped mass by convolving the pressure trace with the theoretical resonance behaviour. The method permits avoiding the spectral problems of the time-frequency transformations by obtaining the trapped mass directly without the need of inferring the frequency content.

Keywords: Trapped mass estimation, Pressure resonance, Combustion diagnosis, Fourier Transform

1. Introduction

In-cylinder pressure has long been used as a powerful tool for engine research and diagnosis [1]. Although for many years restricted to research, the lowering market price of the newest pressure sensors are justifying their frequent implementation [2]. Methods using in-cylinder pressure sensors are of high interest, and many methods are being developed for determining combustion features, e.g. combustion detection [3, 4], noise evaluation [5], air mass estimation [6], emissions control [7], heat transfer [8, 9, 10]...

*Corresponding author
Email address: pabamo@mot.upv.es (Pau Bares)

Most of the algorithms are based on the low frequency pressure trace; however the pressure signal may exhibit significant contents over a broad band of the spectrum, since fast combustion excites the resonance frequencies of the chamber creating pressure oscillations. If excessive, these oscillations can damage the engine, degrade substantially the performance and transmit an excessive high-frequency noise [11, 12].

Traditionally, pressure resonance was investigated to detect knock on SI engines [11, 13]. Knocking is an abnormal combustion on SI engines characterized by the spontaneous ignition of the end-gas, which causes a high release rate exciting heavily the resonance [11, 14, 15] and is a limiting factor for SI engines efficiency. Recently, the development of new combustion modes, based on Homogeneous Charge Compression Ignition (HCCI) [16, 17], has driven the resonance researches on finding useful indexes to quantify the resonance [18, 19, 20]. Although knocking analysis and HCCI resonance are based on the same principles, because of the different chamber conditions, the resonance excitation is substantially different: SI knocking resonance is characterized by high excitation of many modes while HCCI resonance is concentrated on the first circumferential mode [21].

Virtually, all the applications and researches on resonance phenomenon are focused on detecting the resonance frequency (knock detection), locating the resonance to filter it (combustion diagnosis) or trying to quantify the resonance (resonance indexes); most of the applications start from Draper's correlation [22] in order to estimate the resonance frequencies as a function of the speed of sound. Draper's correlation has been demonstrated by many authors by using time-frequency analysis at the pressure signal in order to determine the frequency evolution [23, 24, 25].

Hickling et al. published in 1983 a method for determining the bulk temperature by measuring the period of the resonance pressure oscillation [23], the trapped mass determination was only mentioned as a possible application. Two main problems appear when trying to use the Draper's correlation for inferring the bulk temperature and hence the trapped mass: the variation of the frequency resonance over time, and the determination of the instantaneous frequency.

The variation of the frequency resonance is rooted on the variation of the cylinder geometry with the crankshaft position: the cylindrical assumption of the Drapers correlation is no longer valid when the engine approaches the Top Dead Center (TDC) and only the combustion chamber is left. This problem was addressed by Guardiola et al. [26], who suggested a method for experimentally characterizing the cylinder resonance.

On the other hand, Drapers correlation requires the determination of the instantaneous resonance frequency. In opposition to Hickling et al. manual

method, this must be automated for the real-time implementation of the algorithm. Although Bodisco et al. [27] have discussed the possibility of determining the instantaneous frequency by statistical inference methods, the straightforward solution is using time-frequency analysis (e.g. the Short Time Fourier Transform (STFT) is used in [26]). However, spectral analysis imposes an elevated computational burden, and does not necessarily calculate the actual instantaneous frequencies: there is no method capable of obtaining the real time-frequency content [28], but the solution depends on the transform used (Wigner, STFT, etc.). The goal of the paper is the development of a direct time-to-mass transformation including the resonance behaviour inside the signal transform.

The paper is organized as follows: the experimental layout, whose data will be used along the paper for demonstration purposes, is presented in Section 2; Section 3 will introduce the basics of determining the trapped mass through the pressure resonance, while section 4 will be focused on the determination of the instantaneous frequency through some of the most common time-frequency transformations (WD and STFT). This will serve for illustrating the resonance behaviour, and for identifying the main drawbacks associated to each of these transformations. The new direct transformation will be described in Section 5, where it will be compared with the aforementioned spectral transformations, as with the classical sensing methods for trapped mass determination. Finally, last section sums up the contributions of the new transform.

2. Experimental layout and test data

The tests were developed on a single cylinder Reactivity Controlled Compression Ignition (RCCI) engine [29]. The engine was equipped with gasoline port injection and diesel direct injection, allowing multiple diesel injections during the cycle. EGR facilitated the control of the engine over different combustion modes, while electrohydraulic variable valve timing (VVT) permitted controlling the valves to change the mass instantaneously at transient tests. The pressure was measured with a Kistler 6125c sensor and processed by a National Instruments RT-PXI acquisition system, with a resolution of 5 samples/deg. The main characteristics of the engine are summarized in table 1.

Pressure signal was crank angle based acquired. On one hand, time based acquisition is more precise to estimate frequencies but on the other hand, crank angle based acquisition permits locating the signal during the combustion cycle and this is specially important when using the volume in the calculations (because volume is a function of the crank angle).

Some tests were focused on detecting the instantaneous engine speed during the cycle: the pressure was acquired crank angle based and the time between samples was measured by an onboard clock (80MHz). The engine speed variation was bounded bellow 5 % on medium load. For simplicity the engine speed

was considered constant, consequently time evolution (t) or crank angle evolution (α) will be used indiscriminately along the paper.

Table 1: Main engine characteristics

Displaced volume (V_d)	1806cc
Engine speed (n)	1200 rpm
Bore (D)	123.6 mm
Combustion mode	RCCI-Diesel
Pressure samples/degree (s_n)	5
In-cylinder pressure sensor	Kistler 6125c

Even though all tests were conducted at the same engine speed due to test bench requirements, the only limitation of the method is the Nyquist frequency ($F_s/2 \geq f_{res}$). Then, if the pressure measurement is crank angle based, the frequency acquisition (F_s) depends on the engine speed and the encoder resolution:

$$F_s = \frac{360n}{60} s_n = 36 \text{ kHz} \geq 2f_{res} \tag{1}$$

Considering the maximum range of the first mode of resonance frequency for this engine (up to 6 kHz) and the encoder resolution, the minimum admissible engine speed would be 400 rpm, which is clearly below idle speed.

Ringing Intensity (RI) index proposed by Eng [21]:

$$RI = \frac{0.05}{2\gamma} \left[\frac{\delta p}{\delta t}\right]_{max} \frac{\sqrt{\gamma R T_{max}}}{p_{max}} \tag{2}$$

was used to quantify the resonance. 5 MW/m^2 was determined as the limit for allowable ringing [20, 30].

In order to provide a reference estimation of the trapped air mass, a classical procedure combining several measurements and models was used. This procedure will be referred hereinafter as the auxiliary method, and will be compared with the in-cylinder pressure based estimation.

The auxiliary method was based on the direct measurement of the air mass flow through hot film anemometry, the determination of EGR by means of CO_2 balance in the intake manifold, the measurement of the blow-by using the orifice measuring principle, and the determination of the fuel mass flow by a fuel balance. In order to estimate the residual gas fraction and the short circuit mass flow, an emptying-and-filling model as in [31, 32, 33] was used for solving the flow through the engine valves.

Test campaign consisted on 54 steady operation points, where trapped mass and the resonance excitation was modified by varying the actuators (injected fuel mass, injection timing, engine load, boost pressure and EGR rate). Measured RI and the trapped mass as calculated by the auxiliary method for all the tests are plotted on figure 1.

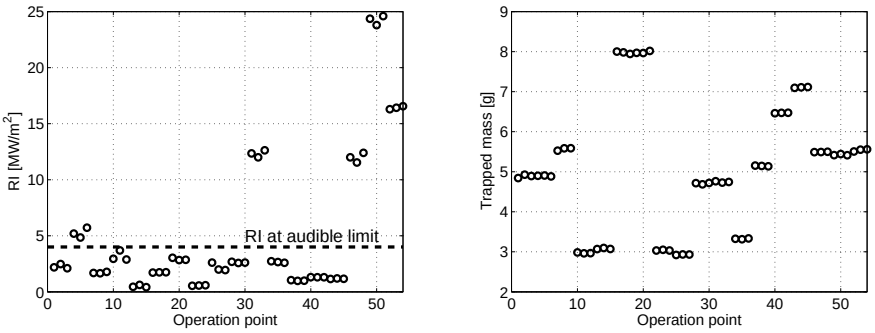

Figure 1: Ringing intensity and sensed trapped mass over the tested points

In order to illustrate the transient behaviour of the method, two tests were performed. In the first one boost pressure was smoothly varied from 2 bar to 2.7 bar, while in the second a sharp step was applied to the intake valve closing, from -190^o to -235^{o}CAD.

3. From resonance to trapped mass

Draper, on 1938, established the bases of the resonance on combustion chambers by solving the wave equation with cylindrical contour conditions [22]. As a consequence, he obtained a relation between the engine speed (a) and the resonance frequency ($f_{i,j}$) as a function of the bore (D) and the correspondent Bessel constant($B_{i,j}$): the axial modes ($g = 1, 2...\infty$) can be neglected because next to the TDC the frequencies are too elevated ($h \approx 0$).

$$f_{i,j} = a\sqrt{\frac{B_{i,j}^2}{(\pi D)^2} + \frac{g^2}{(2h)^2}} = \frac{aB_{i,j}}{\pi D} \tag{3}$$

However, the theoretical Bessel constants do not fit the resonance problem of a combustion chamber with bowl, specially near the TDC. Figure 2 shows the theoretical resonance frequency of the first mode over a spectral distribution (WD): the experimental resonance frequencies obtained seem to converge to the cylindrical approach far from the TDC, but when the piston approaches the TDC the cylindrical assumption does not longer hold. The influence of the bowl has been demonstrated by CFD studies, such as [34], where different bowl

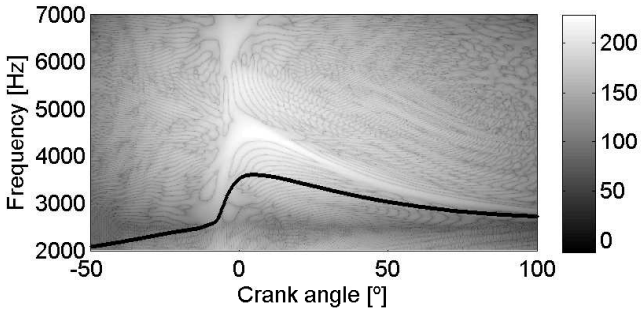

Figure 2: Theoretical Bessel constants (Black line) over a Spectral distribution of the pressure signal (WD)

geometries were numerically simulated to predict its resonance response.

In order to estimate the resonance of a chamber with bowl, the resonance is assumed to be a function of the speed of sound in the chamber but also of the geometry. As the geometry does only change with the crank angle evolution, a crank angle varying coefficient must be added to take into account the bowl perturbation (Eq. 4).

$$B^c_{i,j}(\alpha) = \mu(\alpha) B_{i,j} \tag{4}$$

where $\mu \approx 1$ when the piston is far from the TDC.

Once the relation between the speed of sound and the resonance frequency is calibrated, the resonance frequency can be simplified as a function of the cycle evolution (α) and the trapped mass (m): the in-cylinder properties can be calculated by assuming the ideal gas law ($pV = mRT$), the instantaneous volume of the chamber (V) can be estimated by geometry parameters, and R can be accurately obtained with temperature regressions [35] or by control oriented estimations [36].

$$f_{i,j}(\alpha, m) = \frac{\mu(\alpha) B_{i,j} \sqrt{\gamma(\alpha, m^*) p(\alpha) V(\alpha)}}{\pi D \sqrt{m}} \tag{5}$$

At this point, in opposition to the majority of the works, C.Guardiola et al. proposed the inversion of the problem: instead of calculating the resonance frequency through the mass, a powerful tool is calculating the trapped mass through the resonance frequency. C.Guardiola et al. proposed using the STFT to estimate the instantaneous frequency and assuming complete combustion for the calculations [26]. A sketch of the trapped mass calculation by using STFT is shown in figure 3.

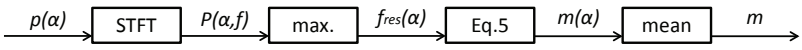

Figure 3: Trapped mass calculation by the STFT method

4. Time-frequency analysis

To discern the resonance frequencies on a given signal $s(t)$, the signal must be viewed on the frequency domain. Frequency domain representation was initiated by Fourier on 1807 by a transformation consistent on the convolution of the signal with harmonics of constant frequency:

$$S(f) = \int_{-\infty}^{\infty} s(t) e^{-j2\pi f t} dt \tag{6}$$

But Fourier transformation is not sufficient to detect time-varying frequencies on a given signal, therefore is not adequate for automotive piston engines as the pressure resonance frequencies vary with the crankshaft position [25]. The time-frequency analysis, also known as spectral analysis, consists on inferring the density of the signal as a function of the time and the frequency, $P(t, f)$.

However, there are an infinite number of time-frequency distributions that can correlate $s(t)$ and $S(f)$, as sketched in figure 4. Following, a brief review of the most commonly used transformations is given:

- Short Time Fourier Transform (STFT):

  The most widely used method for studying non-stationary signals is the STFT [37, 38], which is calculated through:

$$P_{STFT}(t, f) = |S_t(f)|^2 = \left| \int_{-\infty}^{\infty} s(\tau) h(\tau - t) e^{-j2\pi f \tau} d\tau \right|^2 \tag{7}$$

  It consists on breaking up the signal and separately analyses each piece of the signal. In order to smoothly divide the signal and avoid creating discontinuities, the signal is multiplied by a window function, $s_t(\tau) = s(\tau)h(\tau - t)$. The length and the type of the window (*Blackman-Harris, Hamming...*) directly affect the final transformation and accordingly they must be carefully chosen.

  Since the STFT is analysing a finite time segment of the signal, it is including frequency content of the surrounding instants on the instantaneous frequency. Only when the window length tends to zero the instantaneous

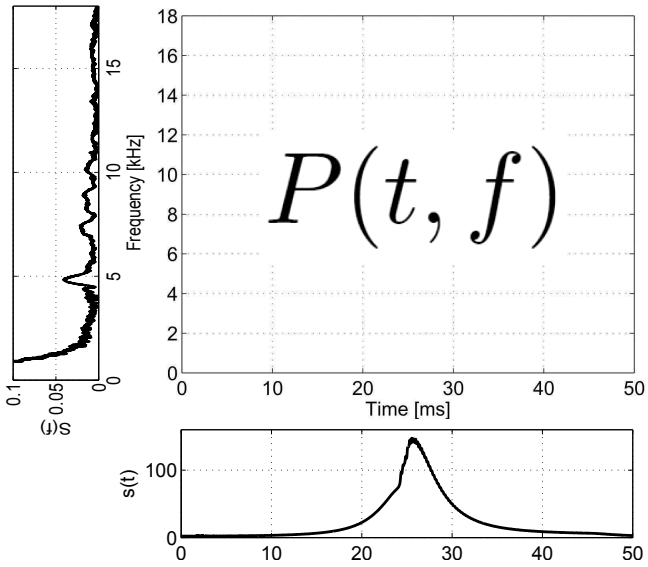

Figure 4: Time-frequency analysis

frequency calculated by Eq. (7) is the actual frequency. But a small window is not necessarily better, since the uncertainty principle establishes that is not possible to afford high bandwidth and high resolution [28]. Narrowing the window implies loosing frequency resolution while broadening the window implies diluting the frequency content. Figure 5, left plot, represents in dB the spectrum of a pressure signal using a STFT with a Blackman-Harris window of 25 CAD.

- Wigner Distribution (WD)

  An alternative of the STFT is the WD, which is built by multiplying the signal at a past time by the signal at a future time. The general form of the WD is calculated as follows:

$$P_{WD}(t,f) = \int_{-\infty}^{\infty} s^*(t - \frac{1}{2}\tau)s(t + \frac{1}{2}\tau)e^{-j2\pi f\tau}d\tau \tag{8}$$

  It can be understood as a folding of the signal over the studied time.

  Right plot in figure 5 plots the Wigner Distribution, in dB, of a pressure signal after a band-pass filter was applied . The main problem of the Wigner Distribution is existence of the cross terms, also known as *ghost terms*, consisting in virtual frequency components caused by the folding of the signal. Practically, the cross terms entail filtering the resonance, because the cross terms of the high amplitude low frequency terms mask the low amplitude high frequency terms, and the signal noise is distributed by

all the frequency components. Some variants of the Wigner Distributions, named as Pseudo-Wigner distributions, are based on windowing the lag to emphasize the signal around the time t [24], nevertheless, some of the desired properties of the Wigner distribution no longer hold, e.g. marginals or instant frequency. When comparing with the STFT, the computational burden discards the WD in most of real time applications.

- Other distributions:

  Other distributions based on the Kernel Method [28], such as Choi Williams distribution [39] or Zhao-Atlas-Marks distribution [40], maintain the desired properties of the WD and reduce the *ghost terms* but at the expense of a significant increment in complexity.

As conclusion, despite WD and other representations' ability to represent the real frequency distribution more precisely, the existence of ghost terms and the computational burden in comparison with STFT rapidity, mainly due to the Fast Fourier Transform (FFT), are the responsible that most of the applications prefer using the STFT. This was also the selection in [26].

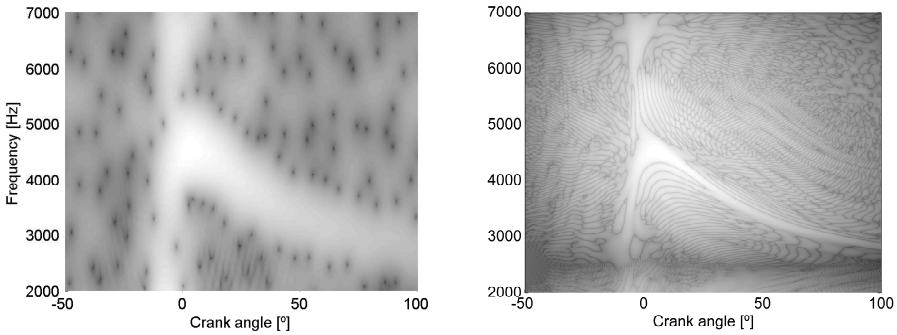

Figure 5: Time-frequency description of a pressure signal: STFT left, WD right

5. Trapped mass transformation

The proposed transformation was developed in order to avoid implementing time-frequency calculations by incorporating Eq. (5). Figure 6 shows the new approximation proposed.

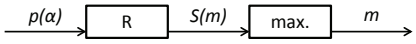

Figure 6: Trapped mass calculation by the new transformation method

Instead of a transformation characterized by different constant frequencies (f), herein is proposed a transformation based on time-varying frequency curves

characterized by the mass (m):

$$S_{i,j}(m) = \int_{-\infty}^{\infty} s(t) e^{-j2\pi \int_{-\infty}^{t} f(\tau,m) d\tau} dt \tag{9}$$

where the phase shift is picked up by the term $\int_{-\infty}^{t} f d\tau$. In constant frequency transformations, such as Fourier transform, this term is simplified as ft.

As the first cylindrical resonance mode is the most representative, specially on HCCI resonance, the transformation should be characterized only by this mode ($B_{1,0} = 1.842$), and equation (9) becomes:

$$S(m) = R[s(t)] = \int_{-\infty}^{\infty} s(t) e^{-j2\pi \int_{-\infty}^{t} \frac{\mu(\tau) B_{1,0} \sqrt{\gamma(\tau) p(\tau) V(\tau)}}{\pi D \sqrt{m}} d\tau} dt \tag{10}$$

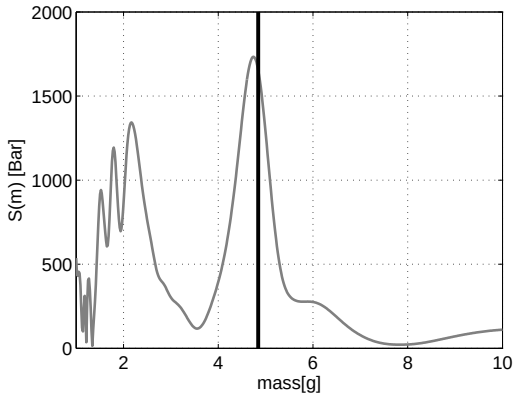

Figure 7: Mass transformation: black line = Mass sensor estimation, grey line = S(m)

Figure 7 is the result of the resonance mass transform over the pressure cycle of figure 4. The low frequency content of the signal is dispersed by the high virtual masses and the other resonance modes ($B_{i,j}$) appear as peaks at punctual virtual masses ($m_{i,j}$):

$$m_{i,j} = m \left(\frac{B_{1,0}}{B_{i,j}} \right)^2 \tag{11}$$

In fact, it is not necessary to use all the signal. Using only a windowed part of the signal, where the resonance surely exists, will reduce the number of operations required. Figure 8 shows the result of the windowed mass transforms moving the window every 0.1 degree. Although the intensity of the transformation is strongly affected by the window position, the black line, correspondent to the maximum peak of the transformation (the actual mass) is almost constant during all the cycle.

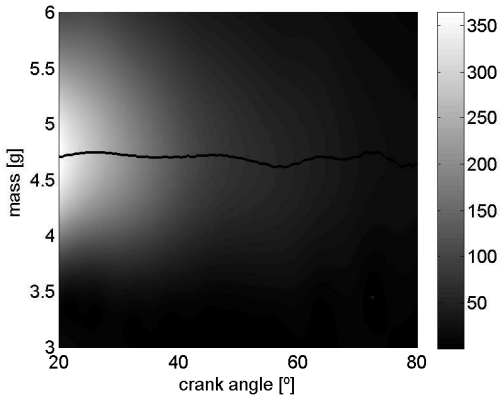

Figure 8: Windowed Mass transformations on different window locations

6. Results and discussion

In order to calibrate the method, some of the tests were run under resonance levels exceeding the advisable values. Twelve operation points were conducted at RI above $10MW/m^2$ (see figure 1) to achieve sufficient excitation and easily processing the frequency components of the pressure signal.

Figure 9 shows the calibration of the bowl resonance by using the WD and the STFT over 12 points, the variation over the operation points is represented by the standard deviation; both, STFT and WD, give similar values, the WD took more time for being calculated but it is more reliable as the window effect on the STFT cause a higher dispersion on the calculation.

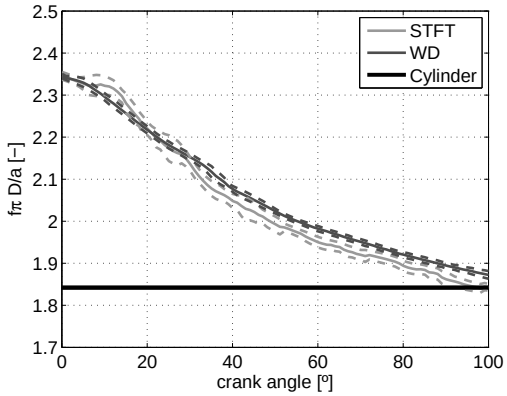

Figure 9: Bowl resonance calibration: – Estimation, - - Estimation $\pm\ \sigma$

The rest of the points were used for validating the method under normal RI. A total of 42 points were used, the combustion was centred between -7^o and 7^o (CA50) and the trapped mass ranged from 2.9 to 8 grams per stroke. A *Blackman-Harris* window of 60^o centred at 30^o was used , and Eq. 7 was discretized as follows:

$$S(m) = T \sum_{\alpha=0}^{\alpha=60} h(\alpha - 30) s(\alpha) e^{-j2\pi T \sum_{\phi=0}^{\phi=\alpha} \frac{\mu(\phi) B_{1,0} \sqrt{\gamma(\phi) p(\phi) V(\phi)}}{\pi D \sqrt{m}}} \tag{12}$$

where T is the sampling period ($T = 1/F_s$).

Figure 10 compares the results of the resonance transform method with the results obtained by the auxiliary method. The method agree perfectly with the auxiliary method, the discrepancies between both methods are even lower than the expected error from sensors, which may reach 5% [41].

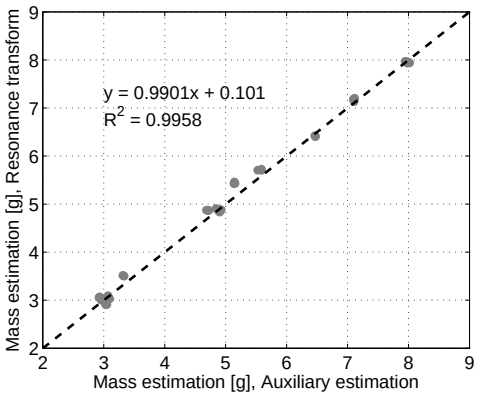

Figure 10: Steady results comparative

In order to present the cycle-by-cycle potential of the method two different transient tests were developed: A smooth variation on the boost pressure and a sudden change on the IVC settings.

Figure 11 shows the boost pressure, the RI and the trapped mass calculation obtained by a smooth boost pressure variation from 2 Bar to 2.7 Bar at 1200 rpm. One important advantage of using resonance for measuring the trapped mass is the cycle-by-cycle resolution. Sensors, such as hot-wire anemometer or blow-by measurements, are limited to measure flow quantities. Oppositely, the resonance of each cycle is considered independent, and then a trustful cycle-by-cycle measurement is possible to obtain by relying on it. Figure 11 demonstrate that under reasonable RI levels (medium plot) the cycle-by-cycle mass values obtained by the new transform (lower plot) are consistent with the boost pres-

sure evolution (upper plot).

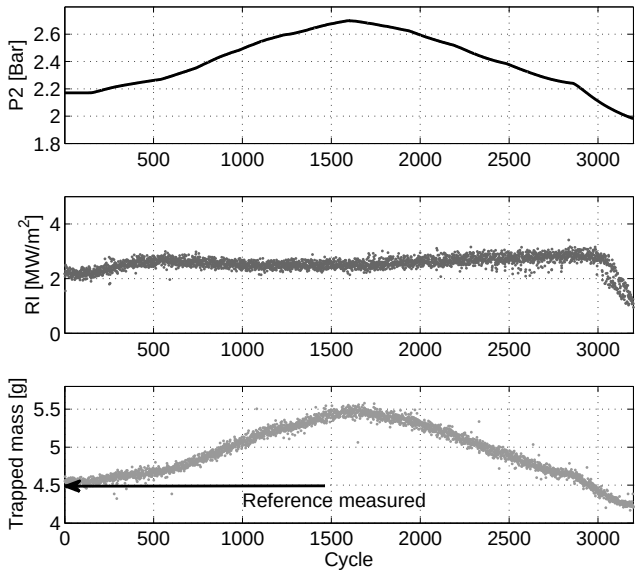

Figure 11: Upper plot: Boost pressure, Medium plot: RI, Lower plot: Reference level measured by the auxiliary method (black line) and trapped mass estimation by the new transform (dots)

Left plot in figure 12 plots the results obtained by the new transform over the IVC step: 3000 pressure cycles were recorded at 1200 rpm and the IVC varied from -190^o to -235^o on the cycle 308 and returned to the steady position on the cycle 2620. An instantaneous change in mass is expected when varying the valve control, however the auxiliary method is only capable of measuring steady points, as a consequence only two measures of the auxiliary method are available (the lower level and at the upper level). Figure 12 plots the individual trapped mass measurements (dots), and an averaged signal based on a 10 cycles window (grey line).

Actually, the valve step data was also used on [26] to demonstrate the capabilities of the STFT method. Right plot in figure 12 shows the results of the new mass transform versus the results obtained by using the STFT. Although the measures were comparable, the new transform improves substantially the computational time because does not obtain the full 2D spectral content. Furthermore, it avoids STFT problems and discard automatically the faulty measures when the mass peak is not sufficiently higher.

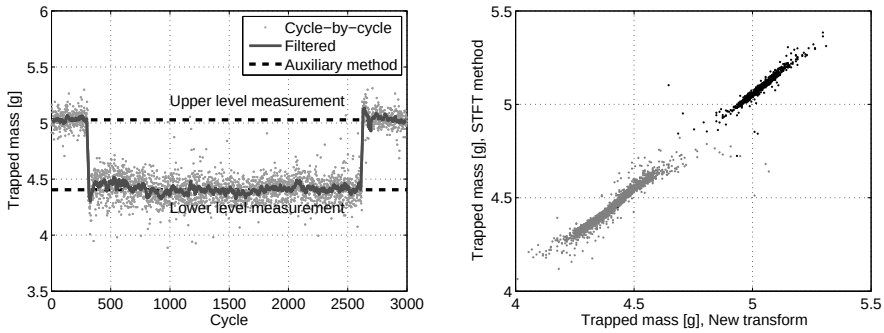

Figure 12: Trapped mass measurement over an instantaneous IVC step (left) and comparative with STFT method (right)

7. Conclusions

Fourier transform and time-frequency distributions have been widely used for evaluating the pressure resonance on reciprocating engines. However, Fourier transform is based on a transformation of a signal into constant frequency harmonics and a time-frequency analysis, such as STFT or WD, are needed in order to detect the resonance frequency evolution. This paper incorporates the resonance behaviour in a frequency varying transformation (Eq. 7), avoiding time-frequency distributions. The method uses virtual masses for the new domain, transforming the trapped mass on a peak in the virtual mass domain. The method was tested on a four-stroke RCCI engine over steady points and the cycle-by-cycle potential of the method was illustrated on transient tests.

On the authors' opinion, relaying on the resonance instead of conventional trapped mass estimations imply several advantages, being the most relevant:

- Fewer sources of error: The method permits a measure of the trapped mass by using the pressure signal and an hypothesis of initial composition. The few signals used ensure obtaining small sensor errors at the final measure.
- One cycle resolution: The resonance of one cycle is considered independent of each combustion event, as a consequence, the method developed permits one cycle resolution without using flow assumptions.

And incorporating a new transform for the resonance analysis permits:

- Reducing the number of operations: This directly reduces the problem to one dimension and permits using only a part of the signal.
- Higher precision and robustness: As there is no need for obtaining the time-frequency spectrum, the method is not affected by time-frequency analysis complications, e.g. ghost terms on the WD or window function interference on the STFT.

References

[1] A. Randolph. Cylinder-pressure-based combustion analysis in race engines. *SAE paper 942487*, 1994.

[2] J. D. Powell. Engine control using cylinder pressure: Past, present, and future. *Journal of Dynamic Systems, Measurement and Control, Transactions of the ASME*, 115(2 B):343–350, 1993.

[3] J. M. Luján, V. Bermdez, C. Guardiola, and A. Abbad. A methodology for combustion detection in diesel engines through in-cylinder pressure derivative signal. *Mechanical Systems and Signal Processing*, 24(7):2261–2275, 2010.

[4] M. Baratta and D. Misul. Development and assessment of a new methodology for end of combustion detection and its application to cycle resolved heat release analysis in ic engines. *Applied Energy*, 98:174–189, 2012.

[5] F. Payri, A. Broatch, B. Tormos, and V. Marant. New methodology for in-cylinder pressure analysis in direct injection diesel engines - application to combustion noise. *Measurement Science and Technology*, 16(2):540–547, 2005.

[6] J. M. Desantes, J. Galindo, C. Guardiola, and V. Dolz. Air mass flow estimation in turbocharged diesel engines from in-cylinder pressure measurement. *Experimental Thermal and Fluid Science*, 34(1):37–47, 2010.

[7] M. Beasley, R. Cornwell, P. Fussey, R. King, A. Noble, T. Salamon, A. Truscott, and G. Landsmann. Reducing diesel emissions dispersion by coordinated combustion feedback control. *SAE paper 2006-01-0186*, 2006.

[8] A. J. Torregrosa, P. Olmeda, J. Martn, and C. Romero. A tool for predicting the thermal performance of a diesel engine. *Heat Transfer Engineering*, 32(10):891–904, 2011.

[9] J. M. Desantes, A. J. Torregrosa, A. Broatch, and P. Olmeda. Experiments on the influence of intake conditions on local instantaneous heat flux in reciprocating internal combustion engines. *Energy*, 36(1):60–69, 2011.

[10] C. A. Finol and K. Robinson. Thermal modelling of modern engines: A review of empirical correlations to estimate the in-cylinder heat transfer coefficient. *Proceedings of the Institution of Mechanical Engineers, Part D: Journal of Automobile Engineering*, 220(12):1765–1781, 2006.

[11] X. Zhen, Y. Wang, S. Xu, Y. Zhu, C. Tao, T. Xu, and M. Song. The engine knock analysis - an overview. *Applied Energy*, 92:628–636, 2012.

[12] D. Scholl, C. Davis, S. Russ, and T. Barash. The volume acoustic modes of spark-ignited internal combustion chambers. *SAE paper 980893*, 2005.

[13] A. Hettinger and A. Kulzer. A new method to detect knocking zones. *SAE paper 2009-01-0698*, 2009.

[14] G. Shu, J. Pan, and H. Wei. Analysis of onset and severity of knock in si engine based on in-cylinder pressure oscillations. *Applied Thermal Engineering*, 51(1-2):1297–1306, 2013.

[15] HG. Brecq and O. Le Corre. Modeling of in-cylinder pressure oscillations under knocking conditions: Introduction to pressure envelope curve. *SAE paper 2005-01-1126*, 2005.

[16] X. Lu, D. Han, and Z. Huang. Fuel design and management for the control of advanced compression-ignition combustion modes. *Progress in Energy and Combustion Science*, 37(6):741–783, 2011.

[17] R. Stanglmaier and C. Roberts. Homogeneous charge compression ignition (hcci): Benefits, compromises, and future engine applications. *SAE paper 1999-01-3682*, 1999.

[18] E. Corti and D. Moro. Knock indexes thresholds setting methodology. *SAE paper 2007-01-1508*, 2007.

[19] N. Cavina, E. Corti, G. Minelli, Moro D., and L. Solieri. Knock indexes normalization methodologies. *SAE paper 2006-01-2998*, 2005.

[20] M. Sjöberg and J.E. Dec. Effects of engine speed, fueling rate, and combustion phasing on the thermal stratification required to limit hcci knocking intensity. *SAE paper 2005-01-2125*, 2005.

[21] J. A. Eng. Characterization of pressure waves in hcci combustion. *SAE paper 2002-01-2859*, 2002.

[22] C.S. Draper. The physical effects of detonation in a closed cylindrical chamber. Technical report, National Advisory Committee for Aeronautics, 1938.

[23] R. Hickling, D. A. Feldmaier, F. H. K. Chen, and J. S. Morel. Cavity resonances in engine combustion chambers and some applications. *Journal of the Acoustical Society of America*, 73(4):1170–1178, 1983.

[24] L. Stankovi and J. F. Bhme. Time-frequency analysis of multiple resonances in combustion engine signals. *Signal Processing*, 79(1):15–28, 1999.

[25] B. Samimy and G. Rizzoni. Mechanical signature analysis using timefrequency signal processing: Application to internal combustion engine knock detection. *Proceedings of the IEEE*, 84(9):1330–1343, 1996.

[26] C. Guardiola, B. Pla, D. Blanco-Rodriguez, and P. Bares. Cycle by cycle trapped mass estimation for diagnosis and control. *SAE Int. J. Engines*, 7(3), 2014.

[27] T. Bodisco, R. Reeves, R. Situ, and R. Brown. Bayesian models for the determination of resonant frequencies in a di diesel engine. *Mechanical Systems and Signal Processing*, 26(1):305–314, 2012.

[28] *Time-Frequency Analysis*. Prentice-Hall, New York, 1995.

[29] J. Benajes, S. Molina, A. Garca, E. Belarte, and M. Vanvolsem. An investigation on rcci combustion in a heavy duty diesel engine using in-cylinder blending of diesel and gasoline fuels. *Applied Thermal Engineering*, 63(1):66–76, 2014.

[30] M. Sjöberg, J. Dec, A. Babajimopoulos, and D. Assanis. Comparing enhanced natural thermal stratification against retarded combustion phasing for smoothing of hcci heat-release rates. *SAE paper 2004-01-2994*, 2004.

[31] F. Payri, J. Galindo, J. Martín, and F.J. Arnau. A simple model for predicting the trapped mass in a di diesel engine. *SAE paper 2007-01-0494*, 2007.

[32] J. W. Fox, W. K. Cheng, and Heywood J. B. A model for predicting residual gas fraction in spark-ignition engines. *SAE paper 931025*, 1993.

[33] P. K. Senecal, J. Xin, and Reitz R. D. Predictions of residual gas fraction in ic engines. *SAE paper 962052*, 1996.

[34] A. J. Torregrosa, A. Broatch, X. Margot, V. Marant, and Y. Beauge. Combustion chamber resonances in direct injection automotive diesel engines: A numerical approach. *International Journal of Engine Research*, 5(1):83–91, 2004.

[35] M. Lapuerta, O. Armas, and J. J. Hernández. Diagnosis of di diesel combustion from in-cylinder pressure signal by estimation of mean thermodynamic properties of the gas. *Applied Thermal Engineering*, 19(5):513–529, 1999.

[36] P. Tunestål. Self-tuning gross heat release computation for internal combustion engines. *Control Engineering Practice*, 17(4):518–524, 2009.

[37] A. Chen and X. Dai. Internal combustion engine vibration analysis with short-term fourier-transform. In *Proceedings - 2010 3rd International Congress on Image and Signal Processing, CISP 2010*, volume 9, pages 4088–4091, 2010.

[38] K. Akimoto, H. Komatsu, and A. Kurauchi. Development of pattern recognition knock detection system using short-time fourier transform. In *IFAC Proceedings Volumes (IFAC-PapersOnline)*, volume 7, pages 366–371, 2013.

[39] H. Choi and W. J. Williams. Improved time-frequency representation of multicomponent signals using exponential kernels. *IEEE Transactions on Acoustics, Speech, and Signal Processing*, 37(6):862–871, 1989.

[40] Y. Zhao, L. E. Atlas, and R. J. Marks. Use of cone-shaped kernels for generalized time-frequency representations of nonstationary signals. *IEEE Transactions on Acoustics, Speech, and Signal Processing*, 38(7):1084–1091, 1990.

[41] F. Payri, S. Molina, J. Martín, and O. Armas. Inuence of measurement errors and estimated parameters on combustion diagnosis. *Applied Thermal Engineering*, 26:226–236, 2005.